Use of sonomicrometry demonstrates the link between prey capture kinematics and suction pressure in largemouth bass

Christopher P. J. Sanford[1],* and Peter C. Wainwright[2]

[1]Department of Biology, 114 Hofstra University, Hempstead, NY 11549, USA and [2]Section of Evolution and Ecology, University of California, Davis, CA 95616, USA

*Author for correspondence (e-mail: christopher.p.sanford@hofstra.edu)

Summary

Suction feeding in fishes is the result of a highly coordinated explosive expansion of the buccal cavity that results in a rapid drop in pressure. Prey are drawn into the mouth by a flow of water that is generated by this expansion. At a gross level it is clear that the expansion of the buccal cavity is responsible for the drop in pressure. However, attempts using high-speed video recordings to demonstrate a tight link between prey capture kinematics and suction pressure have met with limited success. In a study with largemouth bass *Micropterus salmoides*, we adopted a new technique for studying kinematics, sonomicrometry, to transduce the movement of skeletal elements of the head during feeding, and synchronized pressure recordings at a sampling rate of 500 Hz. From the positional relationships of six piezoelectric crystals we monitored the internal movements of the buccal cavity and mouth in both mid-sagittal and transverse planes. We found that peak subambient pressure was reached very early in the kinematic expansion of the buccal cavity, occurring at the time when the rate of percentage change in buccal volume was at its peak. Using multiple regression analyses we were consistently able to account for over 90%, and in the best model 99%, of the variation in buccal pressure among strikes using kinematic variables. Sonomicrometry shows great promise as a method for documenting movements of biological structures that are not clearly visible in the external view provided by film and video recordings.

Key words: sonomicrometry, kinematics, feeding, buccal pressure, largemouth bass, *Micropterus salmoides*.

Introduction

Feeding in fishes has become one of the most extensively studied areas of vertebrate functional morphology (for a review, see Ferry-Graham and Lauder, 2001). From the early studies of function based on morbid anatomy (e.g. Gregory, 1933; Tchernavin, 1948), to mechanical models (Muller et al., 1982; Muller, 1996; Cheer et al., 2001), and a diversity of technology employed by experimental functional morphologists (Osse, 1969; Lauder, 1980a,b; Sanderson et al., 1994), we have gained numerous insights into both the biomechanics of prey capture and the evolution of functional design using fish feeding as a model. Yet, in spite of this success, a number of fundamental problems in fish feeding have eluded researchers. One of these is a clear understanding of the connection between the complex actions of the musculoskeletal system of the skull and the pressures generated inside the buccal cavity during suction feeding.

The teleost skull is highly kinetic and involves some 60 skeletal units powered by approximately 80 muscles (Winterbottom, 1974). Suction feeding is the result of a rapid expansion of the buccal cavity (Van Leeuwen, 1984; Lauder, 1985) that generates a pressure gradient, and water is accelerated into the mouth opening to fill the expanding buccal

cavity (Muller et al., 1982; Muller and Osse, 1984; Van Leeuwen, 1984). Pressure and water motion are intimately related in this process. Suction pressure is generated by two phenomena (Muller et al., 1982). Expansion of the buccal cavity occurs rapidly and may be the largest cause of depressed buccal pressure. In addition, the induced water flow generates a smaller subambient pressure, which is added to that induced by buccal expansion. Prey are carried into the oral cavity by the flow generated during the suction process. The velocity of flow entering the mouth, and hence the magnitude of the pressure drop, are expected to be proportional to rate of volume change of the fish's mouth (Muller et al., 1982; Van Leeuwen and Muller, 1983). The induced flow velocity is considered to be a key component of suction feeding performance, and since flow and pressure are intimately related, understanding how fish modulate suction pressure is an important step in one of the fundamental goals of fish feeding biomechanics: to understand the basis of suction feeding performance.

Several studies have empirically investigated functional correlates of buccal pressure, including muscle activation patterns (Lauder et al., 1986; Grubich and Wainwright, 1997) and cranial kinematics (Svanbäck et al., 2002). The overall

pattern that has emerged from these studies is one in which muscle activity and cranial kinematics (excluding significant interindividual effects) typically account for less than 55% of the variation in pressure patterns among feeding attempts. This moderately weak relationship is disappointing because the water flow generated by buccal expansion is mechanically linked to buccal pressure (Muller et al., 1982). The lack of tight relationships between muscle activity patterns (EMGs), kinematics and buccal pressure may be the result of a faulty understanding of the mechanical basis of buccal pressure; alternatively, previous attempts to describe the relevant kinematic events with data derived from video recordings may not have portrayed key motions accurately. One reason to suspect the latter is that video recordings offer only an external view, and thus provide only indirect estimates of buccal cavity expansion. In the present study we employed sonomicrometry to measure buccal cavity expansion during suction feeding by largemouth bass. Sonomicrometry uses ultrasound to precisely measure distances between small (approximately 2.0 mm) piezoelectric crystals. By attaching these crystals to key structures in the walls of the buccal cavity we were able to obtain an accurate picture of changes in the dimensions of the buccal cavity and jaw motion during suction feeding. Kinematic variables generated from positional data were used in multiple regression analyses, with dependent variables taken from simultaneous buccal pressure recordings. There are no studies to date that have attempted to directly measure internal expansion of the buccal cavity during suction feeding. Furthermore, empirical investigations of the relationship between kinematics and pressure suggest that peak gape, for example, precedes minimum subambient pressure (Lauder, 1980c).

Our experiments were designed to answer three questions about suction feeding in largemouth bass: (1) what is the temporal relationship between kinematics of the internal surfaces of the buccal cavity and the subambient pressures generated by those movements; (2) what are the temporal relationships between various elements of the buccal cavity during suction feeding; and (3) can kinematics of the internal buccal cavity be used to accurately predict buccal pressures?

Materials and methods

The largemouth bass (*Micropterus salmoides* Lacepede) is the largest piscivorous member of the Centrarchidae, a group of approximately 30 species of North American freshwater fishes. *Micropterus* was selected as the experimental animal because it has been the subject of several previous analyses of feeding functional morphology (Lauder, 1983; Norton and Brainerd, 1993; Richard and Wainwright, 1995; Wainwright and Richard, 1995), as well as two studies aimed at linking musculoskeletal action with suction pressure (Grubich and Wainwright, 1997; Svanbäck et al., 2002). These studies have established that this species employs a wide range of kinematics and pressure profiles while feeding. *Micropterus* was also chosen because the buccal cavity of this species is

large, facilitating the implantation of sonomicrometry crystals and a pressure transducer with a quick recovery time.

Specimens

The largemouth bass were obtained from a private fish farm in Yolo County, CA, USA. Specimens were housed individually in 100 l aquaria at 23–25°C and were fed a mixed diet of goldfish (*Carassius auratus*), mosquitofish (*Gambusia affinis*) and pieces of squid (*Loligo opalescens*). The specimens used for this study were identified as Individuals 1–5 and had a standard length of 235, 242, 249, 257 and 265 mm, respectively. A narrow size range was used to reduce any scaling effects that have been demonstrated in this species (Richard and Wainwright, 1995; Wainwright and Richard, 1995).

Before each experiment, the bass were starved for 2–3 days to increase hunger level. Prior to surgery the bass were gradually anesthetized with a light dose of tricaine methanesulfonate (MS-222). The bass were returned to their home tank following surgery (described below). They were allowed to recover overnight and recording of feeding behavior was started the following day. The bass were fed goldfish (*Carassius auratus*), and feeding bouts were recorded in succession over a period of 1–2 days, during which strikes representing a wide range of effort were obtained. The number of strikes obtained for analysis ranged from seven (Individual 3) to 25 (Individual 1). The total number of sequences analyzed was 88.

Sonomicrometry

We used an eight-channel digital sonomicrometer (Sonometrics Corp.) to measure the kinematics of six internal positions on the wall of the buccal cavity (Fig. 1). These positions were selected to reflect the major movements related to volumetric change in the buccal cavity (Lauder, 1985; Muller, 1989; De Visser and Barel, 1998). The locations of the crystals were: (1) the posterior roof of the mouth just ventral to the parasphenoid, and in the same transverse plane as crystals 3 and 4 (below), (2) the anterior roof of the mouth just ventral to the vomer, (3) the left suspensorium just dorsal to the interhyal-suspensorium articulation, (4) the right suspensorium (the same as 3 but on the opposite side), (5) the dorsal surface of the hyoid at the articulation between the basihyal and the first basibranchial (this position was chosen because when the hyoid is depressed, during expansion of the buccal cavity, this crystal will occupy a position approximately in the same plane as crystals 1, 3 and 4), and (6) the mucosa on the anteroventral-most region of the buccal cavity, close to the dentary symphasis.

The piezoelectric crystals used were omnidirectional and either 1 or 2 mm diameter depending on location, although 2 mm crystals gave a more consistent signal. The crystals were sutured to the mucosal layer using surgical thread. Visual inspection ensured that the crystals were securely tied to the mucosal layer. Any crystal showing excessive movement was anchored using a second suture. All crystals were aligned so
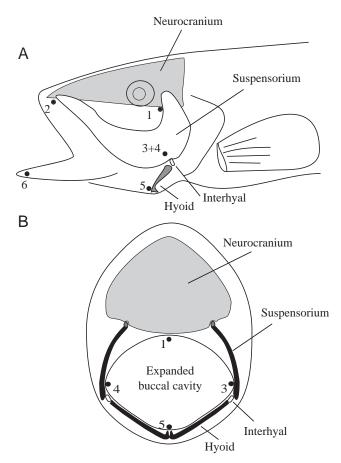
Fig. 1. Schematic view of (A) the lateral head region, and (B) a transverse section through the buccal cavity of the largemouth bass *Micropterus salmoides* to show the placement of sonomicrometric crystals. Crystals are indicated as black dots. See text for discussion of exact locations.

that the tip of the crystal was pointing anteriorly. The wires from the crystals were run anterior to the gill arches (three on each side) and out through the operculum. All six wires were then bundled together and stabilized by suturing them to the skin just anterior to the first dorsal fin.

Sonometric data were recorded using the software program Sonoview (Sonomicrometrics Corp.) at a sample rate of 500 Hz and a transmit pulse of 500 ns with an inhibit delay of 3 mm. This program records absolute distances between all crystal pairs and we selected those combinations that provided the best signals and were relevant to our analysis (below). These traces were cleaned of outliers and corrected for other signal problems using Sonoview. An ASCII output file was then imported into Biopac Lab Pro V. 3.6.5 for deriving the variables used in our analysis.

Kinematics and variables

The following distances were transduced: posterior hyoid (distance between crystals 1 and 5; Fig. 1), anterior hyoid (distance between crystals 2 and 5), suspensorial distance (distance between crystals 3 and 4) and gape (distance between crystals 2 and 6). During the implantation, crystals 1, 2 and 5

were placed as close to the midline as possible and we assumed that depression and elevation of the basihyal and basibranchials was in the mid-sagittal plane. Thus, crystal 5 swung through an arc in the mid-sagittal plane with crystals 1 and 2. This assumption was verified by examination of feeding profiles from each individual bass to confirm that the change in distance between crystals 3 and 5, and crystals 4 and 5, was symmetrical. In addition to these kinematic variables, the buccal cross-sectional area (hereafter abbreviated to buccal area) was also estimated at approximately the position of crystals 1, 3 and 4. We used changes in this variable as a metric of the expansion of the buccal volume because most expansion occurs in the lateral–lateral and dorsal–ventral axes and not in the anterior–posterior axis. Calculation of buccal area was based on an expanding elliptical model of the buccal cavity. With distances between crystals 1–2, 1–5 and 2–5 defining a triangle, it was possible to calculate the vertical distance of the hyoid relative to the roof of the mouth (axis 1–2) as it moved in the mid-sagittal plane (Fig. 1). This distance was used as one axis of the ellipse and suspensorial distance was used as the other.

From plots of these five variables against time (Fig. 2), we derived displacement, temporal and velocity variables for each capture sequence. The following derived variables were used for further analysis: maximum displacement from onset, onset time (relative to peak subambient pressure = t_0), duration, time of peak displacement (relative to t_0), time to peak displacement from onset, and velocity of displacement. Velocity of displacement was calculated using 20% of maximum displacement as the onset time. This procedure eliminated the variable initial stages of displacement kinematics. From our calculations of buccal area we derived two additional variables: the time of peak rate of change in buccal area (relative to t_0), and the time of peak rate of percentage change in buccal area (relative to t_0). For all derived variables we defined the time of minimum buccal pressure as time zero (t_0). This point was unambiguously identified in all feeding sequences and was of very short duration (about 2 ms).

Pressure

During experiments we simultaneously recorded intra-oral buccal pressure using a Millar SPR-407 microcatheter-tipped pressure transducer. During surgical implant of the sonomicrometry crystals (see above) we also inserted a plastic cannula though the mid-dorsal region of the neurocranium between the nostrils and the eyes. The cannula had an expanded end holding it in place against the skin inside the buccal cavity, where it emerged just lateral to the anterior end of the parasphenoid bone. A sleeve of silicon tubing was fitted flush with the skin of the neurocranium and it stabilized the position of the cannula. Following recovery from surgery the pressure transducer was threaded into the cannula so that the tip was flush with the opening of the cannula in the buccal cavity. The transducer leads were sealed around the head of the cannula by a plastic sleeve with a soft plastic core. The analog pressure signal was digitized at 500 Hz through a
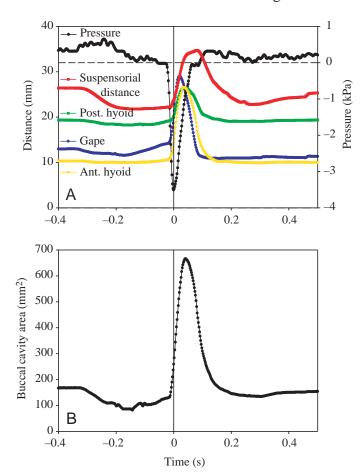
Fig. 2. (A) Representative kinematic profile of buccal cavity variables and pressure during suction feeding in *Micropterus salmoides* to show the overall pattern and preparatory phase (see text). Post., posterior; Ant., anterior. (B) Buccal cavity area plotted against time for the same sequence as in A. Time zero (t_0) represents the time of peak subambient pressure.

parallel channel on the sonomicrometry system, allowing precise synchronization of the two types of data.

The synchronized pressure recordings were also processed in Sonosoft and Biopac Lab Pro V. 3.6.5. From traces of pressure against time we derived the following variables: peak subambient buccal pressure, onset time of the buccal pressure curve (when the pressure fell below ambient), total buccal pressure duration from onset to when the pressure again reached ambient (offset), time to peak subambient buccal pressure, measured from onset to peak subambient buccal pressure, and rate of buccal pressure drop, measured as the average rate from 20% of peak subambient pressure to peak subambient pressure. Again, the 20% onset value was used to calculate rate due to the variable nature of the pressure profile during the initial stages. Finally, pressure area was calculated as the area between ambient pressure and the pressure in the buccal cavity from the onset to the offset of subambient pressure. All experimental techniques were approved by UC Davis (institutional animal care and use protocol #10168).

Statistical analysis

We used multiple-regression analysis to explore the correlations between kinematics of the buccal cavity and pressure. In this analysis we used each pressure variable in turn as the dependent variable and all kinematic variables as the independent variables, adding individual bass as a categorical variable. The resulting analysis of covariance (ANCOVA) model included interaction terms between each kinematic variable and individual bass. Each model was run in a two-step process. Initially, all kinematic variables and interaction terms were included in the model. We then removed variables and interaction terms from the model if their P value was greater than 0.4 (a very conservative cut-off of significance). The reduced model was rerun and although it inevitably provided a lower overall r^2, it is the model reported here. Cumulative r^2 values were calculated to provide insight into the extent to which kinematic variables provided independent explanatory power. All data were $\log_{10}$ transformed prior to data analysis to normalize variances and to linearize exponential relationships. Analyses were performed using Systat for Windows v. 9.

Results

Descriptive kinematics and pressure

The bass were aggressive feeders, using rapid expansion of the buccal cavity (Fig. 2) to generate an average minimum pressure of -5.22 ± 0.28 kPa (mean $\pm$ S.E.M.) (Table 1). Prior to the expansive phase, a preparatory phase where the buccal area decreased by more than 10% was present in 39% of feedings ($N=88$) (e.g. Fig. 2B). Based on plots of buccal area against time (e.g. Fig. 3), the expansive phase lasted an average of 63 ms (Fig. 4). However, peak subambient pressure was reached on average 45 ms prior to peak buccal area (Table 1, Fig. 4). The mean total duration of the feeding cycle, including expansion and compression, was approximately 205 ms.

Gape distance was the first kinematic variable to increase during the expansive phase, with a mean onset time of -40.7 ± 2.7 ms (all values are relative to t_0; Table 1, Fig. 4). Anterior hyoid depression (-26.2 ± 1.8 ms) and posterior hyoid depression (-27.7 ± 2.4 ms) began virtually simultaneously (Table 1). Finally, the suspensorium began to abduct at -19.6 ± 1.8 ms. The drop in buccal pressure started immediately after the onset of hyoid depression at -24.5 ± 2.0 ms. Buccal area showed a detectable increase at -18.4 ± 2.2 ms (Fig. 4). The temporal sequence of mouth opening followed by hyoid depression and then suspensorial abduction was found in 91% of feeding sequences ($N=88$).

One notable feature that was revealed by the synchronized recordings was the very early time of peak subambient buccal pressure during the feeding sequence (Figs 2, 3). Pressure was the fastest variable to reach its peak value from onset (24.5 ± 2.0 ms), and peak subambient pressure occurred on average 24 ms before the first kinematic variable (gape) reached its peak (Table 1, Figs 3, 4). Subambient pressure reached its peak prior to any kinematic variable 100% of the time ($N=88$).

Table 1. *Basic statistics of variables measured from 88 prey capture sequences in five largemouth bass*

Variable	Mean	S.E.M.	Range	Units
Kinematics				
Gape onset	–40.68	2.72	–5 to –147	ms
Time to peak gape	35.18	1.53	16–104	ms
Time of peak gape	23.85	1.20	5–77	ms
Gape peak displacement	19.25	0.56	8.76–31.10	mm
Gape velocity	0.49	0.02	0.13–0.99	$mm\,ms^{-1}$
Gape duration	148.33	5.59	52–294	ms
Ant. hyoid onset	–26.15	1.78	0 to –83	ms
Ant. hyoid time to peak	39.05	1.48	16–94	ms
Ant. hyoid time of peak	35.97	1.45	18–86	ms
Ant. hyoid peak displacement	15.88	0.45	7.25–25.61	mm
Ant. hyoid velocity	0.53	0.03	0.11–1.13	$mm\,ms^{-1}$
Ant. hyoid duration	195.24	5.88	77–365	ms
Post. hyoid onset	–27.73	2.36	–2 to –161	ms
Post. hyoid time to peak	38.06	1.41	18–90	ms
Post. hyoid time of peak	34.53	1.48	14–92	ms
Post. hyoid peak displacement	12.73	0.52	4.07–28.54	mm
Post. hyoid velocity	0.30	0.02	0.07–0.66	$mm\,ms^{-1}$
Post. hyoid duration	206.71	7.48	76–394	ms
Suspensorium onset	–19.58	1.79	8 to –72	ms
Suspensorium time to peak	50.47	1.89	26–118	ms
Suspensorium time of peak	53.05	1.90	24–106	ms
Suspensorium peak displacement	15.88	0.45	7.25–25.61	mm
Suspensorium velocity	0.28	0.01	0.10–0.60	$mm\,ms^{-1}$
Suspensorium duration	227.51	6.61	82–437	ms
Buccal area onset	–18.38	2.24	90 to –55	ms
Buccal area time to peak	42.61	1.91	24–104	ms
Buccal area time of peak	45.25	2.77	22–162	ms
Buccal area peak displacement	741.5	38.1	231.5–1925.4	mm^2
Buccal area velocity	14.75	0.80	2.32–38.51	$mm^2\,ms^{-1}$
Buccal area duration	205.33	8.04	124–422	ms
Time of peak rate of change in buccal area	11.19	0.73	–5–31	ms
Time of maximum rate of percentage change in buccal area	0.56	0.47	–12–12	ms
Pressure				
Subambient pressure onset	–24.49	0.98	–8 to –58	ms
Peak minimum pressure	–5.22	0.28	–1.61 to –14.56	kPa
Rate of pressure drop	–0.25	0.02	–0.07 to –0.86	$kPa\,ms^{-1}$
Pressure area	–237.9	12.5	–68 to –616	$kPa\,ms$
Duration of subambient pressure	116.8	3.8	46–223	ms

Ant., anterior; Post., posterior.
Onset times and time of peak values are relative to t_0 (time of peak subambient pressure).
S.E.M. is –1 standard error of the mean.

Relative to minimum subambient pressure (t_0), the average time of peak rate of change in buccal area was 11.2 ± 0.7 ms (Table 1), and this was significantly different from the peak rate of percentage change in buccal area, which occurred earlier at 0.56 ± 0.47 ms (mixed model analysis of variance, ANOVA; $P<0.001$, d.f. 1,4) (for example, see Fig. 3C,D). The time of peak values for gape, hyoid and suspensorium followed the same temporal sequence found for onset times, and this sequence occurred in 100% of feedings (N=88) (Fig. 4). During the expansive phase, gape peaked first at 23.9 ± 1.2 ms, followed by the anterior and posterior hyoid measurements, which both peaked at approximately 35 ms. Buccal area peaked at 45.3 ± 2.8 ms and, finally, the suspensoria were maximally abducted at 53.0 ± 1.9 ms (Fig. 4). The early peak of the buccal area relative to suspensorial abduction is a consequence of the hyoid (one of the two axes of buccal area) beginning to elevate before the suspensorium has reached peak displacement, which occurred in 99% of feedings (N=88) (Fig. 5). The temporal sequence of peak values for kinematic variables is also illustrated by superimposing the time of peak values for kinematic variables and pressure onto the displacement of the hyoid crystal with
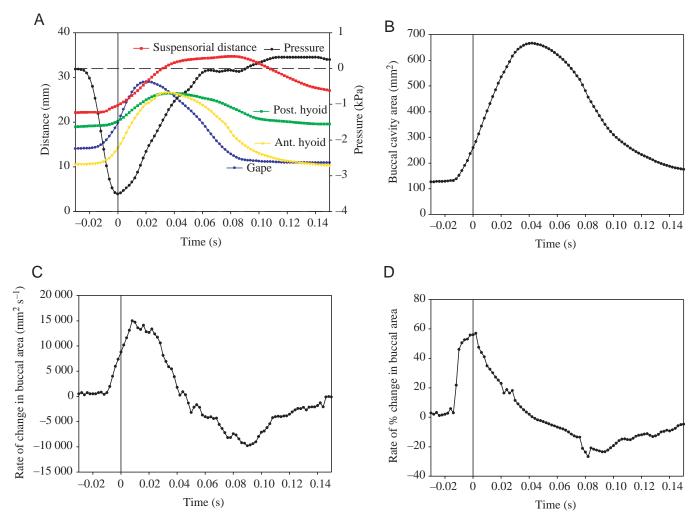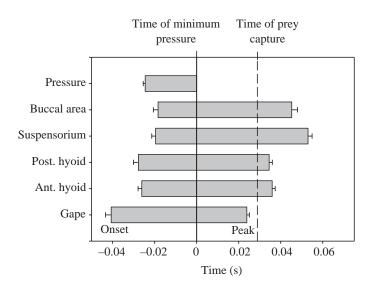
Fig. 3. (A) Representative kinematic profile of buccal cavity variables and pressure to show the details of the expansion phase during suction feeding in *Micropterus salmoides*. Post., posterior; Ant., anterior. (B) Buccal cavity area plotted against time for the same sequence as in A. (C) Rate of change in buccal area for the same sequence as in A. (D) Rate of change in buccal area divided by buccal area for the same sequence as in A. Time zero (t_0, solid vertical line) represents the time of peak subambient pressure. Note the very early time of peak subambient pressure.

reference to the roof of the mouth (defined by fixed crystals 1 and 2) (Fig. 5).

The anterior hyoid measurement had the fastest velocity of any kinematic variable during feeding at 528 ± 25 mm s^{-1} (Table 1), and the correlation of this variable with peak subambient buccal pressure and pressure area is significant (peak subambient buccal pressure, Pearson correlation -0.71, Bonferroni-corrected $P < 0.001$; pressure area correlation 0.48, Bonferroni-corrected $P < 0.05$; also see below). It is important to remember that the displacement of the hyoid is in a

Fig. 4. Bar plot of the mean onset and peak times of variables used in this study. Values are means $\pm$ 1 S.E.M. Time zero (t_0, solid vertical line) represents the time of peak subambient pressure. The vertical dashed line represents the average time of prey capture (i.e. the time that the prey crosses the plane of the gape: 28.83 ± 2.89 ms; mean $\pm$ S.D.), using data from Svanbäck et al. (2002) with similar sized bass. Post., posterior; Ant., anterior.

posteroventral direction and is not restricted to ventral motion only (Fig. 5).

Kinematics and pressure relationships

The multiple regression models were all able to account for over 90% of the variation among strikes in pressure (Tables 2–6). In the reduced multiple-regression models, kinematics accounted for 99.1% of the variation in peak subambient buccal pressure, 96.7% of the variation in buccal pressure area, 91.7% of the variation in buccal pressure rate, 91.9% of the variation in the time to peak buccal pressure, and 96.3% of the variation in buccal pressure duration (Tables 2–6). No single variable or class of variables dominated the regressions. In each multiple regression a large number of variables and interaction terms were independently significant, and no single kinematic variable or interaction term accounted for more than 39.5% of the variance in any pressure variable.

One striking feature of these analyses was the large contribution of the interaction terms in every model. As a group, interactions accounted for 20–45% of the total variance explained by the model (Tables 2–6), which implies that the influence of kinematic variables on pressure varied between individual bass (Fig. 6). In some cases even the direction of the relationship between the
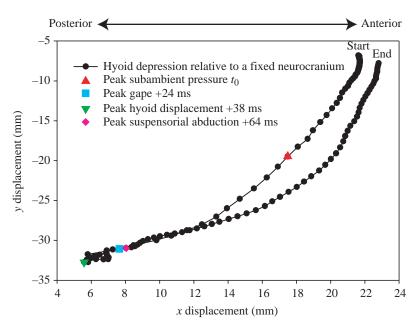

Fig. 5. Typical feeding sequence showing the displacement of the hyoid relative to a fixed neurocranium (top axis). Also indicated are the peak times of all the buccal cavity variables measured in this study. The position of the hyoid was calculated using the distance between crystals 1, 2 and 5 (see Fig. 1). Note the early time of peak subambient pressure (red triangle) relative to kinematic variables. Also note the high velocity at the early stages of depression, as indicated by the spacing between successive points (2 ms intervals).

Table 2. *Results from analysis of covariance from five largemouth bass using kinematic variables as independent variables and peak subambient buccal pressure as the dependent variable*

Variable	d.f.	F-ratio	P	Cumulative r^2	Slope*
Individual	4	3.19	0.017	0.135	
Ant. hyoid velocity	1	64.57	<0.001	0.530	–
Ant. hyoid time to peak	1	53.41	<0.001	0.537	+
Buccal area time to peak	1	40.00	<0.001	0.562	+
Ant. hyoid duration	1	21.33	0.001	0.596	+
Post. hyoid duration	1	19.36	0.002	0.598	+
Gape duration	1	13.75	0.005	0.624	+

Significant interaction terms:[†]
   Ind×a, Ind×b, Ind×c, Ind×d, Ind×e, Ind×f, Ind×g, Ind×h, Ind×i, Ind×j, Ind×k, Ind×l

| Error | 75 | | | | |
| Total cumulative r^2 | | | | 0.991 | |

*Direction of the slope of correlation between the independent variable and dependent variable.

The reduced model of main factors is based on the removal from the larger model of main factors and interaction terms yielding P values of greater than 0.4. See text for details of this analysis.

Ant., anterior; Post., posterior; Ind, Individual.

[†]The interaction terms are listed in ascending order of P value and are coded in Tables 2–6 as: a, buccal area peak displacement; b, ant. hyoid time of peak; c, buccal area time of peak; d, buccal area velocity; e, post. hyoid time of peak; f, ant. hyoid peak displacement; g, post. hyoid duration; h, post. hyoid displacement; I, post. hyoid time to peak; j, suspensorium duration; k, buccal area duration; l, gape peak displacement; m, suspensorium time to peak; n, gape time of peak; o, gape velocity; p, ant. hyoid time of peak; q, suspensorium velocity; r, ant. hyoid duration; s, gape time to peak; t, ant. hyoid velocity; u, suspensorium time of peak; v, gape duration; w, post. hyoid velocity.

Table 3. *Results from analysis of covariance from five largemouth bass using kinematic variables as independent variables and subambient buccal pressure area as the dependent variable*

Variable	d.f.	F-ratio	P	Cumulative r^2	Slope*
Individual	4	7.98	0.001	0.280	
Suspensorium peak displacement	1	30.46	<0.001	0.344	+
Suspensorium velocity	1	26.94	<0.001	0.521	+
Post. hyoid velocity	1	18.62	<0.001	0.543	+
Ant. hyoid velocity	1	17.65	<0.001	0.565	+
Post. hyoid peak displacement	1	16.82	<0.001	0.576	+
Gape peak displacement	1	16.69	<0.001	0.587	+
Gape time to peak	1	10.96	0.003	0.602	+
Gape duration	1	10.95	0.003	0.603	–
Ant. hyoid peak displacement	1	10.94	0.003	0.605	+
Buccal area time to peak	1	5.60	0.027	0.607	–

Significant interaction terms:[†]
    Ind×m, Ind×g, Ind×n, Ind×o, Ind×d, Ind×b, Ind×p

Error	54				
Total cumulative r^2				0.967	

*Direction of the slope of correlation between the independent variable and dependent variable.
Ant., anterior; Post., posterior; Ind, Individual.
See Table 2 and text for details of this analysis.
[†]The interaction terms are listed in ascending order of P value and are coded as indicated in Table 2.

Table 4. *Results from analysis of covariance from five largemouth bass using kinematic variables as independent variables and rate of subambient buccal pressure drop as the dependent variable*

Variable	d.f.	F-ratio	P	Cumulative r^2	Slope*
Individual	4	3.75	<0.001	0.344	
Gape velocity	1	12.06	0.001	0.650	+
Suspensorium duration	1	6.89	0.012	0.676	–
Post. hyoid velocity	1	2.55	0.118	0.729	+
Suspensorium time of peak	1	1.07	0.306	0.732	–
Gape duration	1	0.81	0.372	0.737	–

Significant interaction terms:[†]
    Ind×l, Ind×n, Ind×q, Ind×g, Ind×r, Ind×s, Ind×t

Error	77				
Total cumulative r^2				0.917	

*Direction of the slope of correlation between the independent variable and dependent variable.
Ant., anterior; Post., posterior; Ind, Individual.
See Table 2 and text for details of this analysis.
[†]The interaction terms are listed in ascending order of P value and are coded as indicated in Table 2.

kinematic and pressure variables varied among bass (Fig. 6C), although in none of these cases was the interaction a dominant term in the model.

Discussion

The kinematic patterns associated with suction feeding in fishes have been described in several species (reviewed in Lauder, 1985). However, previous studies have been based on film or video recordings of feeding fish, and only rarely have lateral displacements been reported (e.g. Lauder, 1980a,b; Van Leeuwen and Muller, 1983). Film and video recordings provide only indirect evidence of buccal expansion, and for some variables, such as movement of the hyoid, the relevant structures are mostly obscured by other parts of the skull. Our use of sonomicrometry allowed us to provide the first direct measurements of changes in the internal dimensions of the buccal cavity as we tracked movements of the hyoid and the walls of the suspensoria, and to synchronize these recordings with buccal pressure. We

Table 5. *Results from analysis of covariance from five largemouth bass using kinematic variables as independent variables and time to peak subambient buccal pressure as the dependent variable*

Variable	d.f.	F-ratio	P	Cumulative r^2	Slope*
Individual	4	9.42	<0.001	0.315	
Gape time to peak	1	4.25	0.064	0.429	+
Gape velocity	1	4.25	0.064	0.433	−
Gape peak displacement	1	4.25	0.064	0.461	+
Ant. hyoid time of peak	1	3.43	0.091	0.500	+
Ant. time to peak	1	1.16	0.304	0.507	−
Significant interaction terms:[†]					
Ind×u, Ind×q, Ind×a, Ind×c, Ind×n, Ind×r, Ind×i, Ind×k, Ind×v, Ind×w, Ind×d					
Error	77				
Total cumulative r^2				0.919	

*Direction of the slope of correlation between the independent variable and dependent variable.
Ant., anterior; Post., posterior; Ind, Individual.
[†]The interaction terms are listed in ascending order of P value and are coded as indicated in Table 2.
See Table 2 and text for details of this analysis.

Table 6. *Results from analysis of covariance from five largemouth bass using kinematic variables as independent variables and subambient buccal pressure duration as the dependent variable*

Variable	d.f.	F-ratio	P	Cumulative r^2	Slope*
Individual	4	7.21	<0.001	0.258	
Buccal area peak displacement	1	45.48	<0.001	0.320	+
Buccal area time to peak	1	13.55	0.003	0.420	+
Gape time to peak	1	8.05	0.014	0.532	+
Suspensorium time of peak	1	0.82	0.381	0.586	+
Suspensorium time to peak	1	0.79	0.391	0.595	+
Significant interaction terms:[†]					
Ind×l, Ind×t, Ind×c, Ind×w, Ind×b, Ind×r, Ind×g, Ind×i, Ind×f, Ind×j, Ind×v					
Error	58				
Total cumulative r^2				0.963	

*Direction of the slope of correlation between the independent variable and dependent variable.
Ant., anterior; Post., posterior; Ind, Individual.
[†]The interaction terms are listed in ascending order of P value and are coded as indicated in Table 2.
See Table 2 and text for details of this analysis.

emphasize four major observations on prey capture functional morphology in *Micropterus salmoides* from our analysis. (1) The first direct evidence for the presence of a distinct preparatory phase involving buccal compression immediately prior to the onset of the expansive phase was confirmed and observed in 39% of strike sequences (Fig. 2B). (2) We confirmed that buccal expansion proceeds in an anterior to posterior progression (Figs 2, 3, 4), as described by earlier researchers (Van Leeuwen, 1984). (3) Minimum buccal pressure is achieved early in the strike sequence, 18.4 ms after the initial increase in buccal area, 45 ms prior to peak buccal area (Table 1, Fig. 4), and is synchronous with the time of peak rate of percentage volume change (Fig. 3D). (4) Multiple regression models built with kinematic parameters developed from the sonomicrometric data could account for over 90% of the variation among suction strikes in pressure variables, i.e. with substantially greater success than has been achieved in past studies using video recordings or electromyographic data.

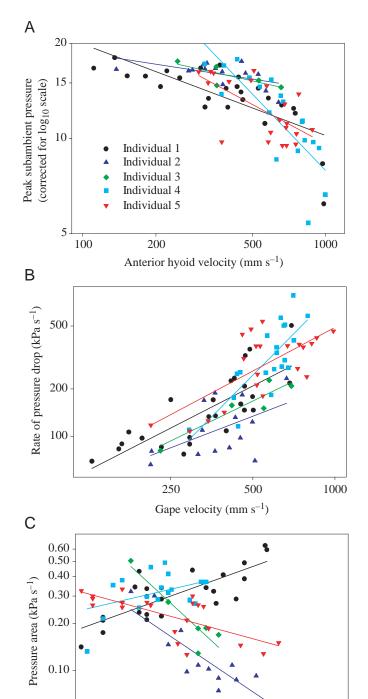*Buccal kinematics during suction feeding*

Previous evidence of a preparatory phase has been limited to periods of superambient pressure prior to suction strikes (Lauder, 1980a,c; Svanbäck et al., 2002) and electrical activity of buccal compression muscles at this time (Liem, 1978; Lauder, 1980a). Gibb (1995) reported a compressive phase in the flatfish *Pleuronichthys verticalis*. However, this was based on movements of the operculum and not the suspensorium. Thus, our study provides the first direct observation of suspensorial adduction and decrease in buccal volume prior to

the expansive phase of suction feeding. In our recordings, following the preparatory phase, the expansive phase began with mouth opening, followed by hyoid depression (about 14 ms later), and then suspensorial abduction (21 ms) (Figs 2A, 4). This kinematic sequence reflects the general models of skull function described in actinopterygians (Lauder and Liem, 1980; De Visser and Barel, 1998; Lauder, 1985). As found previously in analyses of film (Lauder, 1980a,b; De Visser and

Barel, 1998) mouth opening clearly began before hyoid depression or suspensorial expansion (Fig. 2A). We saw no motion of the basihyal crystal relative to the neurocranium (crystals 1 and 2) until 14 ms after the onset of mouth opening, which implies that mouth opening is not initiated by hyoid retraction, as has been proposed by some workers (De Visser and Barel, 1998), but rather by some other action, such as cranial elevation or opercular rotation (Lauder, 1980b; Wilga et al., 2000; Adriaens et al., 2001).

Our results provide empirical evidence that the onset of hyoid depression precedes abduction of the suspensoria (Fig. 4), a pattern that was predicted in models of optimal hyoid motion in cichlids (De Visser and Barel, 1996, 1998). However, this pattern seems to contradict previous electromyographic data from largemouth bass indicating that the levator arcus palatini, a muscle that directly abducts the suspensorium, is activated before the hyoid-retracting sternohyoideus (Wainwright and Richard, 1995; Grubich and Wainwright, 1997).

It has been predicted that the initial stages of hyoid movement are restricted to the longitudinal axis of the body (Aerts, 1991; De Visser and Barel, 1998). By triangulating the two crystals fixed to the roof of the mouth and crystal 5 on the hyoid we were able to calculate movement of the hyoid crystal in the x–y reference frame defined by crystals 1 and 2 (x axis) and crystal 5 (y axis). The resulting pattern shows clearly that the hyoid crystal swings in an arc and does not show an initial retraction along the x axis (Fig. 5). Indeed, in no sequence examined (N=76) was there evidence of an initial retraction of the hyoid crystal.

In *Micropterus*, buccal cross-sectional area continues to increase after the hyoid has reached a maximum, the result of continued suspensorial abduction (Figs 3A,B, 4, 5). Peak buccal area (and presumably volume) is reached about 86 ms after mouth opening. This is approximately 20 ms later than peak volume estimated for *Oncorhynchus mykiss* (Van Leeuwen, 1984). The shorter time to peak buccal volume estimated for *O. mykiss* is unlikely to be related to size, as Van Leeuwen (1984) used larger fish.

It is generally assumed in modeling efforts that during suction feeding the buccal cavity is circular in cross section, thus minimizing the friction forces by creating the lowest

Fig. 6. $\log_{10}/\log_{10}$ bivariate scatterplots with regression lines of correlations between kinematic variables and pressure variables to show (A) and (B) significant main effects with approximately parallel (homogenous) slopes; and (C) a significant interaction effect with regression lines that diverge from one another. Regression equations: (A) individual 1, $y=-0.29x+1.88$, $r^2=0.55$; individual 2, $y=-0.12x+1.50$, $r^2=0.30$; individual 3, $y=-0.17x+1.64$, $r^2=0.67$; individual 4, $y=-0.80x+3.31$, $r^2=0.65$; individual 5, $y=-0.41x+2.22$, $r^2=0.41$; (B) individual 1, $y=0.88x-0.07$, $r^2=0.62$; individual 2, $y=0.66x+0.34$, $r^2=0.26$; individual 3, $y=0.84x-0.35$, $r^2=0.87$; individual 4, $y=1.74x-2.32$, $r^2=0.62$, individual 5, $y=0.91x-0.05$, $r^2=0.49$; (C) individual 1, $y=0.81x-0.55$, $r^2=0.63$; individual 2, $y=-1.52x-2.80$, $r^2=0.71$; individual 3, $y=-2.08x-3.34$, $r^2=0.84$; individual 4, $y=0.53x-0.22$, $r^2=0.28$; individual 5, $y=-0.61x-1.47$, $r^2=0.52$. See text for explanation.

area/circumference ratio (Muller et al., 1982; Barel, 1983; Muller and Osse, 1984; De Visser and Barel, 1998). Although the dorsoventral distance between the hyoid and the roof of the mouth, and the suspensorial distance (Fig. 1), would occasionally be approximately equal, we did not find strong empirical support for this expectation. In most sequences examined, throughout the expansive phase, even at peak hyoid depression, the distance between the hyoid and the roof of the mouth was much less than the distance between the suspensoria. This suggests that the buccal cavity cross-section is described better by a dorsoventrally flattened ellipse than a circle. It might be argued that this inference would depend on the crystals used to calculate buccal area being in the same region of the buccal cavity. Examination of Fig. 5 and displacement patterns of several sequences indicate that, at maximum depression, the hyoid reaches a position almost directly ventral to crystal 1 (see Figs 1, 5). Care was also taken during surgery to place the two suspensorial crystals (3 and 4) in the same transverse plane as crystal 1.

Our discovery of extensive individual variability is common in studies of this type (Tables 2–6; see also Wainwright and Lauder, 1986). These differences between individual bass occurred with both the kinematic variables and the pressure variables.

The relationship between kinematics and pressure

Suction pressure results from the rapid expansion of the buccal cavity in a highly deterministic way that should permit pressure to be accurately calculated from kinematic data (Muller et al., 1982; Muller and Osse, 1984; Van Leeuwen, 1984; Muller, 1989; De Visser and Barel, 1998). However, previous attempts that employed multiple regression methods to link buccal pressure with prey capture kinematics (Svanbäck et al., 2002) and muscle activation patterns (Lauder et al., 1986; Grubich and Wainwright, 1997) in largemouth bass met with only moderate success. Kinematic variables based on movements of the jaws, hyoid and head that were generated from high-speed video recordings accounted for 79.7% of variation in minimum buccal pressure (Svanbäck et al., 2002), although this was reduced to an average of 50% across all pressure variables. Electromyographic variables accounted for an average of 54.8% of the variation among strikes in minimum buccal pressure (Grubich and Wainwright, 1997). In contrast, regressions calculated in the present study were able to account for 99% of the variation between strikes in minimum pressure, and never less than 90% for any pressure variable; these results strongly support the general nature of the kinematic basis of suction pressure (Muller et al., 1982; Muller, 1989). We suggest that one major factor accounting for the statistical resolution of this study compared to that of Svanbäck et al. (2002) was our use of sonomicrometry. This technique allowed us to measure the changes in internal dimensions of the buccal cavity, movements that are directly tied to the increase in buccal volume and hence the flow of water and pressure that are generated. Standard video recordings provide poorer resolution of these movements. The

poorer performance of EMG variables in accounting for buccal pressure may reflect the indirect link between muscle electrical activity and buccal pressure, as compared to a closer link between buccal expansion and pressure.

Although our results provide solid confirmation of the expected relationship between pressure and buccal cavity kinematics, it is not possible to use the multiple regression results to compare the importance of different variables in generating buccal pressure patterns. Independent variables that contribute high r^2 values to the multiple regression models can do so either because they are in fact the causal basis for the buccal pressure dependent variable, or because they are strongly correlated with the actions that do underlie buccal pressure. Further, patterns of shared correlation between independent variables and the dependent variable result in only one of the independent variables making a strong showing in the regression models, while the effect of other variables are not significant because of these correlations (James and McCulloch, 1990). This pattern may actually mask causal relationships between individual variables and can be misleading. For example, anterior hyoid velocity had a significant negative correlation with peak subambient buccal pressure (Fig. 6A). However, we do not regard this as establishing that the movement of the hyoid relative to the vomer is more important in generating peak subambient buccal pressures than any other variable. Anterior hyoid velocity explained approximately 40% of the variation in peak subambient buccal pressure, but at the same time anterior hyoid rate was also significantly correlated with 14 of the possible 24 other variables, not all of which appeared in the reduced multiple regression. Thus, other variables may play a causal role, but are statistically redundant as predictors of buccal pressure. In summary, we emphasize the overall explanatory power of the models, the r^2, rather than the contribution of individual variables.

Although we cannot dissect apart the causal role that individual kinematic variables play in generating buccal pressure, it is of interest that several variables were significant factors in each of the multiple regression models (Tables 2–6). This pattern indicates that the basis of pressure is complex and involves some independence among kinematic variables in their influence on buccal pressure. Svanbäck et al. (2002) in their kinematic study found a consistent pattern of mouth opening and hyoid depression dominating the regression models. Unfortunately, the suspensorial movements were excluded from that study so it is unclear whether these movements would also have contributed significantly to the regression analysis. In our study it is clear that kinematic patterns associated with movements of the hyoid, gape and suspensorium are all contributing at some level to the magnitude of negative buccal pressure. However, in every multiple regression the vast majority of the explanatory power of the kinematics was seen in the first variable. This reflects the strong pattern of coordination, and thus correlation, among kinematic variables.

A conspicuous aspect of the regression analyses was the important role of interaction terms in accounting for the overall explanatory power of the models. The independent variables

were responsible for over half of the variance explained in each multiple regression analysis, but interaction terms accounted for between 20% and 45% of the total variance explained (Tables 2–6). The implication of these interaction terms is that the relationship between individual kinematic variables and pressure often varied among bass (Fig. 6). Unfortunately, it cannot be determined from the regression analyses alone whether this also implies that the kinematic basis of pressure varied among bass. This pattern could also come about if spurious correlations between kinematic variables and pressure are ephemeral and vary among individual fish. However, this result underscores the need for replicated experiments in organismal functional morphology and the pitfalls of relying upon interpretations of results from a single specimen.

Minimum buccal pressure occurred at the time when the rate of percentage volume change in the buccal cavity was highest (Fig. 3D), 11.2 ms before the time of highest rate of increase in buccal area (Table 1). Minimum buccal pressure should occur at the time when the velocity of flow at the pressure transducer is highest. Guided by the principal of continuity we predict that the time of peak subambient pressure would also coincide with the peak flow of water into the mouth. Thus any prey in front of the mouth at the time of peak subambient pressure would be subject to maximum drag generated by the influx of water. We did not directly measure water flow inside the buccal cavity but this flow will be related to the ratio of rate of buccal volume change and the area of the mouth opening. All else being equal, peak flow at the mouth opening will occur when the rate of volume change of the buccal cavity is highest. However, the gape opens during the strike, thus decreasing the relative flow at the mouth opening. The rate of buccal volume change is increasing while the gape is also increasing, which suggests that peak flow may occur at an intermediate point in time, prior to the time of peak volume change, as we observed (Fig. 3).

One implication of this result is that peak subambient buccal pressure was already achieved when many of the kinematic events that were measured occurred. Thus, although variables such as time to peak gape are correlated with minimum pressure, peak gape actually occurs after peak subambient pressure, indicating an indirect mechanical relationship between these variables. The early peak in buccal pressure also indicates that the forces resisting buccal expansion are highest very early in the event and suggest an important role for power production in the expansion muscles of high performance suction events.

References

Adriaens, D., Aerts, P. and Verraes, W. (2001). Ontogenetic shift in mouth opening mechanisms in a catfish (Claridae, Siluriformes): a response to increasing functional demands. *J. Morphol.* **247**, 197-216.

Aerts, P. (1991). Hyoid morphology and movements relative to abducting forces during feeding in *Astatotilapia elegans* (Teleostei: Cichlidae). *J. Morphol.* **208**, 323-345.

Barel, C. D. N. (1983). Towards a constructional morphology of cichlid fishes (Teleostei: Perciformes). *Neth. J. Zool.* **33**, 357-424.

Cheer, A. Y., Ogami, Y. and Sanderson, S. L. (2001). Computational fluid dynamics in the oral cavity of ram suspension-feeding fishes. *J. Theor. Biol.* **210,** 463-474.

De Visser, J. and Barel, C. D. N. (1996). Architectonic constraints on the hyoid's optimal starting position for suction feeding of fish. *J. Morphol.* **228**, 1-18.

De Visser, J. and Barel, C. D. N. (1998). The expansion apparatus in fish heads, a 3-D kinetic deduction. *Neth. J. Zool.* **48**, 361-395

Ferry-Graham, L. and Lauder, G. V. (2001). Aquatic prey capture in ray-finned fishes: A century of progress and new directions. *J. Morphol.* **248**, 99-119.

Gibb, A. C. (1995). Kinematics of prey capture in a flatfish, *Pleuronichthys verticalis*. *J. Exp. Biol.* **198**, 1173-1183.

Gregory, W. K. (1933). Fish skulls: A study of the evolution of natural mechanisms. *Trans. Am. Phil. Soc.* **23**, 71-481.

Grubich, J. R. and Wainwright, P. C. (1997). Motor basis of suction feeding performance in largemouth bass, *Micropterus salmoides*. *J. Exp. Zool.* **277**, 1-13.

James, F. C. and McCulloch, C. E. (1990). Multivariate-analyses in ecology and systematics – panacea or Pandora box? *Ann. Rev. Ecol. Syst.* **21**, 129-166.

Lauder, G. V. (1980a). The suction feeding mechanism in sunfish (*Lepomis*): an experimental analysis. *J. Exp. Biol.* **88**, 49-72.

Lauder, G. V. (1980b). Evolution of the feeding mechanism in Primitive Actinopterygian Fishes: A functional anatomical analysis of *Polypterus*, *Lepisosteus*, and *Amia*. *J. Morphol.* **163**, 283-317.

Lauder, G. V. (1980c). Hydrodynamics of prey capture by teleost fishes. In *Biofluid Mechanics*, vol. 2 (ed. D. Schenk), pp. 161-181. New York: Plenum Press.

Lauder, G. V. (1983). Prey capture hydrodynamics in fishes: experimental tests of two models. *J. Exp. Biol.* **104**, 1-13.

Lauder, G. V. (1985). Aquatic feeding in lower vertebrates. In *Functional Vertebrate Morphology* (ed. M. Hilderbrand, D. M. Bramble, K. F. Liem, and D. B. Wake), pp. 210-229. Cambridge, MA: Harvard University Press.

Lauder, G. V. and Liem, K. F. (1980). The feeding mechanism and cephalic myology of *Salvelinus fontinalis*: form, function, and evolutionary significance. In *Charrs: Salmonid Fishes of the Genus* Salvelinus (ed. E. K. Balon), pp. 365-390. The Netherlands, Junk Publishers.

Lauder, G. V., Wainwright, P. C. and Findeis, E. (1986). Physiological mechanisms of aquatic prey capture in sunfishes: functional determinants of buccal pressure changes. *Comp. Biochem. Physiol.* **84A**, 729-734.

Liem, K. F. (1978). Modulatory multiplicity in the functional repertoire of the feeding mechanism in cichlid fishes. I. Piscivores. *J. Morphol.* **158**, 323-360.

Muller, M. (1989). A quantitative theory of expected volume change in the mouth during feeding in teleost fishes. *J. Zool. Lond.* **217**, 639-662.

Muller, M. (1996). A novel classification of planar four-bar linkages and its application to the mechanical analysis of animal systems. *Phil. Trans. R. Soc. Lond. B* **356**, 689-720.

Muller, M. and Osse, J. W. M. (1984). Hydrodynamics of suction feeding in fish. *Trans. Zool. Soc. Lond.* **37**, 51-135.

Muller, M., Osse, J. W. M. and Verhagen, J. H. G. (1982). A quantitative hydrodynamical model of suction feeding in fish. *J. Theor. Biol.* **95**, 49-79.

Norton, S. F. and Brainerd, E. L. (1993). Convergence in the feeding mechanics of ecomorphologically similar species on the Centrarchidae and Cichlidae. *J. Exp. Biol.* **176**, 11-29.

Osse, J. (1969). Functional morphology of the head of the perch (*Perca fluviatilis* L.): An electromyographic study. *Neth. J. Zool.* **19**, 290-392.

Richard, B. A. and Wainwright, P. C. (1995). Scaling the feeding mechanism of largemouth bass (*Micropterus salmoides*). I. Kinematics of prey capture. *J. Exp. Biol.* **198**, 419-433.

Sanderson, S. L., Cech, J. J. and Cheer, A. Y. (1994). Paddlefish buccal flow velocity during ram suspension feeding and ram ventilation. *J. Exp. Biol.* **186**, 145-156

Sibbing, F. A., Osse, J. W. M. and Terlow, A. (1986). Food handling in the carp (*Cyprinus carpio*): Its movement patterns, mechanisms and limitations. *J. Zool. Lond.* **210**, 161-203.

Svanbäck, R., Wainwright, P. C. and Ferry-Graham, L. A. (2002). Linking

cranial kinematics, buccal pressure and suction feeding performance in largemouth bass. *Physiol. Biochem. Zool.* (in press).

Tchernavin, V. V. (1948). On the mechanical working of the head of bony fishes. *Proc. Zool. Soc. Lond.* **118**, 129-143.

Van Leeuwen, J. L. (1984). A quantitative study of flow in prey capture by rainbow trout, with general consideration of the actinopterygian feeding mechanism. *Trans. Zool. Soc. Lond.* **37**, 171-227.

Van Leeuwen, J. L. and Muller, M. (1983). The recording and interpretation of pressures in prey-sucking fish. *Neth. J. Zool*. **33**, 425-475.

Wainwright, P. C. and Lauder, G. V. (1986). Feeding biology of sunfishes: Patterns of variation in the feeding mechanism. *Zool. J. Linn. Soc.* **88**, 217-228.

Wainwright, P. C. and Richard, B. A. (1995). Scaling the feeding mechanism of largemouth bass (*Micropterus salmoides*). II. Motor pattern. *J. Exp. Biol.* **198**, 1161-1171.

Wilga, C. D., Wainwright, P. C. and Motta, P. J. (2000). Evolution of jaw depression mechanics in aquatic vertebrates: insights from Chondrichthyes. *Biol. J. Linn. Soc.* **71**, 165-185.

Winterbottom, R. (1974). A descriptive synonymy of the striated muscles of the Teleostei. *Proc. Acad. Nat. Sci. Phila* **125**, 225-317.